

Impurities in $s = 1$ Heisenberg Antiferromagnets

Erik S. Sørensen

Department of Physics, Indiana University, Bloomington, IN 47405

Ian Affleck

Department of Physics and Canadian Institute for Advanced Research

University of British Columbia, Vancouver, BC, V6T 1Z1, Canada

(December 20, 1994)

Abstract

The $s = 1$ Heisenberg Antiferromagnet is studied in the presence of two kinds of local impurities. First, a perturbed antiferromagnetic bond with $J' \neq J$ at the center of an even-length open chain is considered. Using the density matrix renormalization group method we find that, for sufficiently strong or weak J' , a bound state is localized at the impurity site, giving rise to an energy level in the Haldane gap. The energy of the bound state is in agreement with perturbative results, based on $s = 1/2$ chain-end excitations, both in the weak and strong coupling limit. In a region around the uniform limit, $J' = J$, no states are found with energy below the Haldane gap. Secondly, a $s = 1/2$ impurity at the center of an otherwise even-length open chain is considered. The coupling to the $s = 1/2$ impurity is varied. Bound states in the Haldane gap are found *only* for sufficiently weak (antiferromagnetic) coupling. For a $s = 1/2$ impurity coupled with a strong (antiferromagnetic) bond, *no* states are found in the Haldane. Our results are in good qualitative agreement with

recent experiments on doped NENP and Y_2BaNiO_5 .

75.10.-b, 75.10.Jm, 75.40.Mg

I. INTRODUCTION

In a seminal paper, Haldane showed that integer spin chains display a gap in the spectrum, where as half-integer spin chains are gapless¹. This was confirmed both by experiments^{2,3} and numerical calculations⁴. Currently, the best estimates of the gap for the isotropic $s = 1$ chain are $\Delta = 0.41050(2)J$, using the density matrix renormalization group (DMRG) method⁵, and $\Delta = 0.41049(2)J$ using exact diagonalization⁶. The dynamical structure factor has also been determined in great detail, by numerical studies of finite systems⁷. Most of the experimental effort has in recent years focused on $\text{Ni}(\text{C}_2\text{H}_8\text{N}_2)_2\text{NO}_2(\text{ClO}_4)$ (NENP) which show clear evidence of the Haldane gap^{3,8}. NENP has not been observed to undergo a three-dimensional ordering at any accessible temperature as opposed to CsNiCl_3 which yielded the first experimental confirmation of the Haldane gap². NENP has a fairly large single ion anisotropy estimated to be $D/J = 0.18^9$ where as CsNiCl_3 is almost isotropic. Recently, experiments have been performed on $\text{Y}_2\text{BaNiO}_5^{10-16}$. This charge-transfer insulator has long one-dimensional chains of Ni atoms at the center of compressed corner sharing oxygen octahedra. Thus, along the chains, the Ni^{2+} ions, with $s = 1$, are separated by nonmagnetic O^{2-} ions. The antiferromagnetic (AF) superexchange interaction between the Ni^{2+} ions is then mediated through the oxygen sites. Y_2BaNiO_5 has a fairly large exchange coupling of $J/k_b = 285\text{K}^{13}-322\text{K}^{11}$, estimated from high temperature susceptibility measurements. From inelastic neutron scattering experiments on powders¹³ it is known that the inter chain coupling is small, $J'/J \ll 10^{-2}$. Thus, the compound is highly one-dimensional and no three-dimensional ordering has been seen. In powder averaged inelastic neutron scattering experiments¹³ two gaps have been observed; For fluctuations parallel to the chain, $\Delta_{\parallel} = 186 \pm 12\text{K}$, and for fluctuations perpendicular to the chain, $\Delta_{\perp} = 99 \pm 6\text{K}$. This is in good agreement with single crystal measurements of $\Delta_{\perp} = 100 \pm 5\text{K}^{14}$. The two gaps are explained in terms of a single ion anisotropy $D/J = 0.16 \pm 0.02^{13}$, a value close to what is found for NENP.

The one-dimensional Haldane gap systems are by now fairly well understood. However,

the important effect of impurities on these systems have only recently been considered. Y_2BaNiO_5 offers several possibilities for doping and is thus well suited for such studies. Non-magnetic Zn^{2+} ions can be substituted for Ni^{2+} , thus effectively severing the Ni chains. Experiments have been performed on Zn doped samples, $\text{Y}_2\text{BaNi}_{1-x}\text{Zn}_x\text{O}_5$ ^{11,14–17}, confirming the picture of chain cutting, with a possibility for an *increase* in the gap with doping¹⁵ due to the fact that the average length of the chain segments is small enough for finite-size effects to be observable. Severing of the chains is predicted to have rather dramatic effects on the low energy excitations. It can be shown that the AF Heisenberg model is fairly well approximated by a valence bond solid (VBS) model¹⁸. The breaking of the valence bonds by the introduction of impurities should produce free $s = 1/2$ spins at the sites next to the impurity. The effect of such free $s = 1/2$ at the chain-ends has been observed in electron-spin-resonance (ESR) experiments on NENP by doping with Cu¹⁹, thereby introducing a $s = 1/2$ at the impurity site, and by doping with non-magnetic Zn, Cd and Hg²⁰. These findings have recently been contrasted by specific heat measurements¹⁷ on $\text{Y}_2\text{BaNi}_{1-x}\text{Zn}_x\text{O}_5$ which show a Schottky anomaly consistent with free $s = 1$.

Another possibility for doping exists in Y_2BaNiO_5 . Carriers, in the form of holes, can be added to the system by replacing the *off-chain* Y^{3+} with Ca^{2+} . DiTusa et. al¹⁶ show, from polarized x-ray absorption spectra, that the added holes are localized on the oxygen *between* the Ni atoms. The addition of a hole on the oxygen sites could effectively turn these into $s = 1/2$ spins, if strongly localized. Ca doping should then have significant effects on the spectrum. Powder averaged inelastic neutron scattering have been performed on $\text{Y}_{2-x}\text{Ca}_x\text{BaNiO}_5$ ¹⁶ showing that Ca doping produces states in the Haldane gap. From analysis of the spectral weight per impurity, DiTusa et al.¹⁶ have proposed that the magnetic disturbance caused by the Ca doping introduces either a triplet or a quartet of subgap bound states.

In order to address the experimental results on doped $s = 1$ spin chains we therefore consider the simple model Hamiltonian

$$H = J \sum_{i=1}^{L/2-1} \{\mathbf{S}_i \cdot \mathbf{S}_{i+1}\} + J \sum_{i=L/2+1}^{L-1} \{\mathbf{S}_i \cdot \mathbf{S}_{i+1}\} + H_{\text{imp}}. \quad (1.1)$$

Here the single ion anisotropy is neglected for simplicity, and \mathbf{S} represents $s = 1$ spins. The impurity Hamiltonian H_{imp} is taken to be either a perturbed bond

$$H_{\text{imp}} = J' \mathbf{S}_{L/2} \cdot \mathbf{S}_{L/2+1}, \quad (1.2)$$

or a $s = 1/2$ impurity, in which case we have

$$H_{\text{imp}} = J' \mathbf{S}_{L/2} \cdot \mathbf{S}' + J' \mathbf{S}' \cdot \mathbf{S}_{L/2+1}, \quad (1.3)$$

where S' is the $s = 1/2$ impurity spin. Schematically the two kinds of impurities are shown in Fig. 1a, 1b, respectively. For the carrier doped compounds Eq. (1.1) may not be a good description and a Hubbard like model may be more appropriate. However, in themselves the Hamiltonians, Eq. (1.1), deserves attention and they should form a good starting point also for the carrier doped compounds if the carriers are strongly localized.

Our approach is to study the low-lying excitations in these systems by comparing large-scale numerical results, obtained using the density matrix renormalization group (DMRG) method, to perturbative results, valid at strong or large coupling, based on effective $s = 1/2$ chain-end excitations generated by broken valence bonds. In section II we discuss the numerical approach. Section III addresses the effects of a single perturbed bond at the center of a chain, while we in Section IV present our results for a $s = 1/2$ impurity. The bulk of our results concerns antiferromagnetically coupled impurities, however, in Sec. V we briefly discuss scenarios for ferromagnetically coupled impurities.

II. NUMERICAL METHODS

We use the density matrix renormalization group (DMRG) method proposed by White^{21–23}. For a detailed discussion of the DMRG method we refer the reader to Refs. 22,23. In all our runs we truncate each half-space to $m = 81$ states, and we work in a subspace defined by the total z-component of the magnetization, S_T^z , and by the parity with respect

to reflection around the central bond, or central spin, for even and odd length chains, respectively. For the DMRG method we therefore denote the different states by $S_T^z P$. Note that, this is the z-component of the spin and *not* the total spin of the state.

The idea behind the DMRG method revolves around the notion of a subsystem, in this case half of the chain, that is strongly coupled to the universe, here the complete chain. As usual in quantum mechanics, the subsystem is then best described by its density matrix, whose eigenvalues give the probability for the subsystem to be in a given eigenstate (of the subsystem density matrix), under the constraint that the universe (the complete chain) is in a given pure state. Here we mean, by pure state, an eigenstate of the Hamiltonian for the complete system. It is now clear that if we start to effectively decouple the subsystem from the universe, by changing the relevant coupling at the center of the chain, the standard DMRG method, where the system is split in half at the impurity site, will become progressively inaccurate. This can be seen in the limit where the coupling to the universe, i. e. the central bond in the chain, is zero, in which case the eigenstates of the density matrix and the Hamiltonian for the subsystem are the same and the DMRG method reduces to standard real space renormalization which is not comparable to the strongly coupled DMRG in precision. We therefore expect to have problems whenever the perturbations that we consider at the center of the chain behave in a way that effectively breaks the system in two. However, as we shall see, this still leaves a workable region where we can obtain useful results. We assume that these difficulties could be overcome by considering more complicated DMRG schemes where the system is not split at the impurity site. However, most other schemes will reduce the symmetry of the problem and we therefore prefer to work with the standard method.

III. BOND DOPING

In the case where the Ni based $s = 1$ Heisenberg antiferromagnets are doped by impurities that form divalent non-magnetic ions, such as Zn, Cd, and Hg, we expect the impurities to

effectively cut the Ni chains. In the valence bond picture¹⁸ this leads to free $s = 1/2$ at the neighboring sites. In this section we consider the more general case where the central bond in an open chain is different from the rest of the chain, although still antiferromagnetic. The Hamiltonian describing the system is Eq. (1.1) and (1.2). For the experiments performed with non-magnetic impurities the relevant situation is that of an extremely weak bond. This can be seen in the experiments of Glarum et al.²⁰ who interpret their results in terms of *free* $s = 1/2$ chain-end spins.

A. Weak Coupling

If the bond at the center of the chain is weak enough we can view the problem as two weakly coupled open chains of half the length. At the end of an open $s = 1$ chain we expect to find an effective $s = 1/2$ excitation, this we shall refer to as a chain-end spin. Thus, for sufficiently long chains, the low-lying excitations can be described by an effective Hamiltonian of two weakly coupled chain-end spins. This should be valid once the coupling of the chain-end spins across the impurity bond is larger than the coupling *along* the chain segment. The latter is known to decrease exponential with the length of the chain segment^{19,24,25}, and should thus quickly become negligible. Experimentally this is the relevant situation for NENP, since it is difficult to obtain high Zn doping levels²⁰, and the average chain segment is therefore likely to be long. Y_2BaNiO_5 offer the possibility of higher doping levels. If we denote by $\mathcal{P}^{(1/2)}$ the projection onto the $s = 1/2$ subspace, we can write $\mathcal{P}^{(1/2)}\mathbf{S}_{s=1}\mathcal{P}^{(1/2)} = \alpha\mathbf{S}''_{s=1/2}$. We need to determine α . Fortunately, an estimate can easily be obtained by looking at the expectation value one of the spins at the *end* of a *free* chain. If we by $|1\rangle$ denote the state that has both the chain-end spins polarized in the “up”-state we find

$$\begin{aligned} \langle 1|\mathbf{S}_{s=1}^z|1\rangle &\simeq \langle 1|\mathcal{P}^{(1/2)}\mathbf{S}_{s=1}^z\mathcal{P}^{(1/2)}|1\rangle \\ &= \alpha \langle 1|\mathbf{S}_{s=1/2}^{z''}|1\rangle = \frac{\alpha}{2}. \end{aligned} \tag{3.1}$$

Previous work^{22,25} have established that $\langle 1|\mathbf{S}_{s=1}^z|1 \rangle \simeq 0.5320$ at the end of a free chain, and thus $\alpha \simeq 1.0640$. The effective Hamiltonian can then be written as

$$H_{\text{eff}} = \alpha^2 J' \mathbf{S}''_{L/2} \cdot \mathbf{S}''_{L/2+1} \quad J' \ll J, \quad (3.2)$$

where \mathbf{S}'' denotes a $s = 1/2$ spin. We then immediately see that the low energy spectrum will be given by a ground-state singlet and a higher lying triplet, the splitting between the two given by

$$\Delta E = \alpha^2 J', \quad J' \ll J. \quad (3.3)$$

This corresponds to a bound state in the Haldane gap, Δ . For the isotropic antiferromagnetic Heisenberg model that we are studying here we have $\Delta = 0.4105J$ in the absence of any impurities. In Fig. 2 we show the energy gap between the two lowest lying states for a chain that has a weak bond of $J' = J/10$ in the middle of an otherwise isotropic chain. Since we have two essentially free $s = 1/2$ chain-end spins at each end of the open chain, the ground-state becomes four-fold degenerate. For finite chain lengths we expect these two chain-end spins to combine into a ground-state singlet, 0^+ , with an exponentially low-lying triplet, 1^- ^{26,25}. In the thermodynamic limit the triplet and the singlet become degenerate. Thus, if we want to calculate the spectrum caused by the impurity we need to look at higher excited states. The resulting gap, which remain finite in the thermodynamic limit, can be calculated between the 2^+ and 1^- states, where we for computational convenience take the 1^- state to represent the ground-state since they become degenerate in the thermodynamic limit. As is clearly evident in Fig. 2, the gap converges quickly to a value of $\Delta E = 0.1141$. With $J' = 0.1J$ we find that Eq. (3.3) gives $\Delta E = 0.1132$ in excellent agreement. The good agreement between the perturbative results and the DMRG results lends further support to the picture of effective $s = 1/2$ chain-end spins.

The DMRG method is convenient for studying correlations in real-space. In Fig. 3 we show the expectation value of the z-component of the spin along a 100 site chain for $J' = 0.1J$. In the 2^+ state we have effectively polarized all four $s = 1/2$ chain-end spins

at sites 1, 50, 51, and 100 in the “up” direction. In order to focus attention on the effects of the impurity we have subtracted off $\langle S_i^z \rangle_{1-}$. In the 1^- state the chain-end spins at site 50, 51 are combined into a singlet, by subtracting off $\langle S_i^z \rangle_{1-}$ we therefore cancel out the effect of the chain-end spins at site 1 and 100. One sees that the two chain-end spins surrounding the perturbed bond have effectively formed a localized state.

Using the DMRG method we can now map out the energy of this bound state as a function of the weak coupling, J' . Due to the problems mentioned in Section II it is not possible to treat values of J' below $J/10$ within the standard DMRG. However, since the impurity state is localized, the convergence to the thermodynamic limit is very fast as can be seen in Fig. 2. Our results are shown in Fig. 4. The filled squares are the numerical results, the solid line the Haldane gap for the isotropic chain, $\Delta/J = 0.41050$, and the dashed line indicates the result from Eq. (3.3). From Fig. 4 it is seen that only for $J' < 0.7J$ does a bound state below the isotropic Haldane gap exist. Around $J' = 0.7J$ the bound state seen in Fig. 3 delocalizes and spreads out over the entire chain. This is shown in Fig. 5 where we plot $\langle S_i^z \rangle_{2+} - \langle S_i^z \rangle_{1-}$ as a function of chain index i for a 100 site chain with $J' = 0.7J$. Clearly this state is not localized and it resembles what one finds for the isotropic chain²⁶. We therefore conclude that it is necessary to weaken the central bond below a critical value $J'_c \text{ weak} \approx 0.7J$ in order to create a bound state.

B. Strong Coupling

We now turn to a discussion of the opposite limit where the central bond is very strong, $J' \gg J$. For the antiferromagnetic coupling that we consider here, the two neighboring spins will be contracted into a singlet. In the limit $J' \rightarrow \infty$ the chain will be severed as was the case for a weak bond. We now want to derive an effective Hamiltonian valid for $J' \gg J$. As a starting point it is convenient to consider the case where we only have four spins described by the Hamiltonian:

$$H = JS_1 \cdot S_2 + J'S_2 \cdot S_3 + JS_3 \cdot S_4. \quad (3.4)$$

We do perturbation theory in J/J' . Note that when $J = 0$ there is a degeneracy since the spins, \mathbf{S}_1 and \mathbf{S}_4 can be in arbitrary states. This is lifted in second order perturbation theory in J . The result of second order perturbation theory can be expressed in terms of an effective Hamiltonian acting on the low-energy subspace, in which \mathbf{S}_2 and \mathbf{S}_3 are projected onto the singlet state:

$$H_{\text{eff}} = PH' \frac{1}{E_0 - H_0} H' P. \quad (3.5)$$

Here

$$H_0 \equiv J' \mathbf{S}_2 \cdot \mathbf{S}_3, \quad (3.6)$$

$$H' \equiv J \mathbf{S}_1 \cdot \mathbf{S}_2 + J \mathbf{S}_3 \cdot \mathbf{S}_4, \quad (3.7)$$

and P projects onto the singlet ground-state of H_0 , with energy $E_0 = -2J$. Acting with H' on the ground-state of H_0 produces the eigenstate of H_0 with spin 1 and energy, $E_1 = -J$.

Thus:

$$\begin{aligned} H_{\text{eff}} &= \frac{J^2}{-J'} P (\mathbf{S}_1 \cdot \mathbf{S}_2 + \mathbf{S}_3 \cdot \mathbf{S}_4)^2 P \\ &= \text{constant} - \frac{2J}{J'} P (\mathbf{S}_1 \cdot \mathbf{S}_2) (\mathbf{S}_3 \cdot \mathbf{S}_4) P \\ &= \text{constant} - \frac{2J}{J'} \langle 0 | S_2^a S_3^b | 0 \rangle S_1^a S_4^b, \end{aligned} \quad (3.8)$$

where $|0\rangle$ denotes the spin-0 ground-state of H_0 . Using:

$$\langle 0 | S_2^a S_3^b | 0 \rangle = \frac{1}{3} \delta^{ab} \langle 0 | \mathbf{S}_2 \cdot \mathbf{S}_3 | 0 \rangle = -\frac{2}{3} \delta^{ab}, \quad (3.9)$$

we obtain:

$$H_{\text{eff}} = \frac{4}{3} \frac{J^2}{J'} \mathbf{S}_1 \cdot \mathbf{S}_4. \quad (3.10)$$

The same calculation applies to a chain of arbitrary length. H_{eff} now contains all the additional couplings which don't involve the pair of strongly coupled spins, $\mathbf{S}_{L/2}$ and $\mathbf{S}_{L/2+1}$ ie.:

$$H_{\text{eff}} = J \sum_{i=1}^{L/2-2} \mathbf{S}_i \cdot \mathbf{S}_{i+1} + J \sum_{i=L/2+2}^{L-1} \mathbf{S}_i \cdot \mathbf{S}_{i+1} + \frac{4}{3} \frac{J^2}{J'} \mathbf{S}_{L/2-1} \cdot \mathbf{S}_{L/2+2}. \quad (3.11)$$

This is exactly the same as the original Hamiltonian of Eq. (1.1) with two sites removed from the ends of the chain and J' replaced by $4J^2/3J'$. Assuming this impurity coupling is much smaller than J we write an effective low-energy Hamiltonian by proceeding along the lines of Section III A. By introducing spin-1/2 variables, $\mathbf{S}_{L/2-1}''$ and $\mathbf{S}_{L/2+2}''$, we obtain:

$$H_{\text{eff}} = \frac{4}{3} \frac{J^2}{J'} \alpha^2 \mathbf{S}_{L/2-1}'' \cdot \mathbf{S}_{L/2+2}''. \quad (3.12)$$

From this effective Hamiltonian we can then derive a simple expression for the bound state:

$$\Delta E = \frac{4}{3} \alpha^2 \frac{J^2}{J'}, \quad J' \gg J. \quad (3.13)$$

We have calculated the gap $\Delta E = E_{2+} - E_{1-}$ as a function of the coupling, J/J' , to the $s = 1/2$ impurity spin. Our results, extrapolated to the thermodynamic limit, are shown in Fig. 6. The solid line indicates the Haldane gap, $\Delta/J = 0.41050$, for the pure chain. The solid squares are the numerical results obtained using the DMRG method. The dashed line denotes the perturbative result Eq. (3.13). The open circles indicate a direct diagonalization of Eq. (3.4) with \mathbf{S}_1 and \mathbf{S}_4 spin one-half. As explained in Section II we are limited to study $J/J' \geq 0.25$. For $J/J' = 0.5$ the limiting value of the gap is very close to the value of the isotropic chain, Δ , and for $J/J' \leq 0.5$ there appears to be no bound state in the Haldane gap. For smaller J/J' a bound state emerges, and we see good agreement between the numerical results and the effective Hamiltonian Eq. (3.12). As was the case for a weak bond we find a critical coupling, $J/J'_{\text{c strong}}$, but now with an approximate value of $J/J'_{\text{c strong}} \approx 0.5$ above which no bound state occurs.

The picture of a quenched singlet in the middle of the chain weakly coupled to two chain-end spins on either side, can be substantiated by calculating the expectation value of the z-component of the spin along the chain. This is shown in Fig. 7 for $L = 100$, $J/J' = 0.25$. Again we have subtracted off the 1^- state configuration. The quenched singlet is clearly visible at the center of the chain and we see a large signal from the two polarized chain-end

spins at $i = L/2 - 1$ and $i = L/2 + 2$. Since one site has effectively been removed from each of the two half-chains Fig. 7 appears inverted with respect to Fig. 3. At the point where the bound state disappears we again find that the expectation value $\langle S_i^z \rangle_{2+} - \langle S_i^z \rangle_{1-}$ spreads out over the entire chain.

We may think of a magnon as behaving, in many respects, like an ordinary particle of mass $m = \Delta/v^2$, where v is the spin-wave velocity. Thus it may, at first, seem surprising that no bound state exists for a weak perturbation of the coupling, $J' \approx J$ since there is a well-known theorem of one-dimensional quantum mechanics which states that an attractive potential always produces a bound state, no matter how weak it is²⁷. Our result is not surprising if one looks in a bit more detail at the mapping of the spin problem into an effective one-particle quantum mechanics problem.

We represent the spin operators at long length-scales in terms of the non-linear σ (NL σ) model field, ϕ (obeying the constraint $|\phi|^2 = 1$) and the associated canonical momentum, $\mathbf{l} = (1/vg)\phi \times \partial\phi/\partial t$, as:

$$\mathbf{S}_i \approx s(-1)^i \phi + \mathbf{l}. \quad (3.14)$$

The Hamiltonian density becomes:

$$\mathcal{H} = \frac{vg}{2} \mathbf{l}^2 + \frac{v}{2g} \left(\frac{d\phi}{dx} \right)^2. \quad (3.15)$$

Acting on the vacuum, ϕ creates the triplet of single-magnon states. A local perturbation in the exchange couplings leads to additional local terms in the field theory Hamiltonian density of the form:

$$\delta\mathcal{H} = vV(x) \left(\frac{d\phi}{dx} \right)^2 + V'(x) \mathbf{l}^2, \quad (3.16)$$

where $V(x)$ and $V'(x)$ are some short-range functions. Note that we *do not* get simply $V(x)\phi^2$, since this term is trivial due to the constraint, $\phi^2 = 1$.

We sometimes approximate the NL σ model by a free massive field theory model with Hamiltonian density²⁸:

$$\mathcal{H} \approx \frac{v}{2}\mathbf{\Pi}^2 + \frac{v}{2}\left(\frac{d\phi}{dx}\right)^2 + \frac{\Delta}{2v}\phi^2, \quad (3.17)$$

where the constraint on ϕ is now relaxed and $\mathbf{\Pi}$ is the associated cononical momentum.

This gives the dispersion relation:

$$E = \sqrt{\Delta^2 + (vk)^2}. \quad (3.18)$$

(We have shifted the wave-vector by π .) We may easily treat the additional impurity term, $vV(x)(d\phi/dx)^2$. This gives the Schrödinger equation:

$$-(1/2)\psi'' - [V(x)\psi']' = mE\psi. \quad (3.19)$$

We obtain this equation for each of the three magnon polarizations. Note that this *does not* correspond to a standard potential scattering term. We could obtain a potential scattering term from a term in the NL σ model Hamiltonian of the form $V(x)(\phi^z)^2$ or $V(x)l^z$. However, these terms break the $SU(2)$ symmetry and therefore can't appear in the Heisenberg model. The latter term corresponds to a local magnetic field. The former could arise if we have a crystal field term in addition to the Heisenberg exchange.

The peculiar derivative potential term does not necessarily lead to a bound state if it is weak. To demonstrate this we consider the case of a step function:

$$\begin{aligned} V(x) &= 0 \quad (|x| > a) \\ V(x) &= -V_0 \quad (|x| < a). \end{aligned} \quad (3.20)$$

Solutions to the Schrödinger equation will have discontinuous ψ' at $x = \pm a$. Defining $\psi'(a^\pm)$ to be the limit of $\psi'(x)$ as $x \rightarrow a$ from above or below respectively and similarly for $\psi'(-a^\pm)$ we obtain:

$$\begin{aligned} \psi'(a^+) &= \psi'(a^-)[1 - 2V_0] \\ \psi'(-a^-) &= \psi'(-a^+)[1 - 2V_0]. \end{aligned} \quad (3.21)$$

The important thing to notice is that if $V_0 < 1/2$, the derivative does not change sign at the discontinuity. There can then be no solution which vanishes at $x \rightarrow \pm\infty$. This follows

since, assuming an even wave-function, it must have the form $\cosh[\sqrt{2|E|m/(1-2V_0)}x]$ for $|x| < a$ which is increasing as we move away from 0. It has to turn into $\exp[-\sqrt{2|E|m}|x|]$ for $|x| > a$. This can't happen without a change in sign of the derivative. [ψ itself must be continuous.] Alternatively, we could assume an odd wave-function but we have the same problem. If $V_0 > 1/2$, there is a solution. It is an odd function of x ; a sine function for $|x| < a$. The binding energy is determined by:

$$\tan \sqrt{\frac{2|E|m}{2V_0-1}}a = \sqrt{2V_0-1}. \quad (3.22)$$

This has a solution for all $V_0 > 1/2$. As $V_0 \rightarrow 1/2^+$, we get:

$$|E|m \rightarrow (2V_0-1)^2/2a^2. \quad (3.23)$$

This provides a counter-example to the statement that there is always a bound state for a weak derivative potential term. On the other hand, there is a rigorous proof of the fact (see, for example Ref. 27) for an ordinary potential term. This argument is admittedly quite incomplete since we haven't analyzed the other, $V(x)\mathbf{I}^2$ term, nor dealt carefully with the passage from the NL σ model to the free model. (This additional term seems to give a type of non-linear Schrödinger equation.) Ignoring these complications, and assuming that the step function result is universal, the above argument suggests that as $J' \rightarrow J'_c$ the critical coupling where the bound state disappears, the binding energy behaves as:

$$E_b \propto (J' - J'_c)^2. \quad (3.24)$$

This is not inconsistent with our numerical results, but substantially more numerical work for J' close to J'_c would be needed in order to verify this dependence.

Our findings in this section are in disagreement with a recent Schwinger-Boson calculation²⁹.

IV. $S = 1/2$ IMPURITIES

We now turn to a discussion of $s = 1/2$ impurities in a $s = 1$ AF Heisenberg chain. Experimentally two scenarios have been studied. First, Cu^{2+} ($s = 1/2$) was substituted for

Ni^{2+} ($s = 1$) in NENP¹⁹. Here, the introduced $s = 1/2$ impurity structurally takes the same place as the original Ni ion. Experimentally one finds a weak *ferromagnetic* coupling to the neighboring chain-end spins¹⁹. Secondly, carriers were added to Y_2BaNiO_5 by substituting Ca for Y. DiTusa et al.¹⁶ argue that the holes become localized on the O sites between the Ni ions. Here the situation is different since the introduced $s = 1/2$ impurity does *not* take the place of a $s = 1$, instead, it is placed *between* two Ni ions. Thus, the superexchange between the two Ni ions is broken and presumably replaced by a *direct* exchange to the $s = 1/2$, J' , which is likely to be large compared to J . Aharony et al.³⁰ have argued that for $\text{La}_{2-x}(\text{Sr},\text{Ba})_x\text{CuO}_{4-y}$ the analogous coupling should be large, $|J'| \gg |J|$. However, the appropriate sign and value of J' for a simple linear chain Heisenberg model capable of describing the experiments on $\text{Y}_{2-x}\text{Ca}_x\text{BaNiO}_5$ ¹⁶ is an open question. In the following we shall limit our discussion to the case of an antiferromagnetic coupling, $J' > 0$.

A. Weak Coupling

Following the approach in Section III A, for a weak bond at the center of the chain, we can try to find an effective Hamiltonian for a weakly coupled $s = 1/2$ impurity at the center of the chain. In this case we again view the sites $L/2$ and $L/2 + 1$ of the $s = 1$ chain as being occupied by chain-end spins that effectively behave as if they were spin one-half. By projecting onto the $s = 1/2$ subspace we represent the chain-end spins at these two sites by $\alpha\mathbf{S}''$, where \mathbf{S}'' is now a real spin one-half. We then obtain an effective low energy Hamiltonian. With \mathbf{S}' representing the $s = 1/2$ impurity spin we have:

$$H_{\text{eff}} = \alpha J' [\mathbf{S}''_{L/2} \cdot \mathbf{S}' + \mathbf{S}' \cdot \mathbf{S}''_{L/2+1}]. \quad (4.1)$$

The spectrum for this effective Hamiltonian consists of a ground-state doublet and an excited doublet and quadruplet. The ground-state doublet has $S^P = 1/2^+$, and energy $E = -\alpha J'$. The excited doublet, $S^P = 1/2^-$, has energy $E = 0$. Finally, the quadruplet, $S^P = 3/2^+$, has energy $\alpha J'/2$. From this effective Hamiltonian we see that we should have *two* low-lying levels with energies in the Haldane gap with energies given by

$$\Delta E_{1/2^-} = \alpha J', \quad (4.2)$$

and

$$\Delta E_{3/2^+} = \frac{3}{2}\alpha J'. \quad (4.3)$$

For a weak *ferromagnetic* coupling we would have obtained $\Delta E_{1/2^-} = \alpha J'/2$, $\Delta E_{1/2^+} = 3\alpha J'/2$.

In order to observe these two levels with the DMRG method we need to determine the relevant quantum numbers for the complete system. We begin by considering the case where the two half-chains surrounding the $s = 1/2$ impurity are of *even* length. We consider the situation where the chain-end spins at sites $L/2$ and $L/2 + 1$ are coupled weakly with a coupling g , $g \ll J'$, to the chain-end spins at the sites 1 and L , respectively. Since the chain segments have an *even length* this coupling, g , is *antiferromagnetic*²⁵. It is now straight forward to obtain the level diagram shown in Fig. 8a. If the two half-chains have an *odd length* the coupling, g , is *ferromagnetic*²⁵ and we obtain the level diagram shown in Fig. 8b. Note that, since we in either case have an even number of valence bonds we do not get a change of parity from the rest of the chain. Thus, we see that in the thermodynamic limit the ground-state is eight-fold degenerate with an eight-fold and sixteen-fold degenerate level above it. In our implementation of the DMRG method we cannot use the total spin as a good quantum number but only the total z-component. In order to determine the two levels given by Eqs. (4.2) and (4.3) we then see from Fig. 8 that we need to calculate the energy differences $E_{3/2^-} - E_{3/2^+}$ and $E_{5/2^+} - E_{3/2^+}$. Only for $L/2$ odd is $3/2^+$ the true ground-state. The Haldane gap to bulk excitations (i. e. excitations not localized at the center and/or ends of the chain) will be between the $5/2^-$ and $3/2^+$ states.

In Fig. 9 we show the energy gap, $\Delta E(L)$, as a function of chain length L , for a $s = 1$ chain with a $s = 1/2$ impurity. The coupling to the $s = 1/2$ impurity is $J' = 0.2J$. The symbols denote the gaps: $E_{5/2^-}(L) - E_{3/2^+}(L)$ (triangles) to the state $5/2^-$ (Haldane gap), $E_{5/2^+}(L) - E_{3/2^+}(L)$ (squares) to the state $5/2^+$, and $E_{3/2^-}(L) - E_{3/2^+}(L)$ (circles) to the state $3/2^-$. Clearly, we have two low-lying excitations well separated from the Haldane gap.

For the $3/2^-$ state we find the gap to be $0.2073J$, compared to $0.2128J$ from Eq. (4.2). Although at large L we have minor problems with the numerical results for the $5/2^+$ state we can also in this case estimate the gap to ~ 0.31 which compares favorably to the result 0.3192 from Eq. (4.3).

It is also possible to study the spatial extension of the bound states. However, as opposed to Section III, $\langle S_i^z \rangle$ for the state $3/2^+$ is non-zero across the impurity site. It is therefore difficult to give a quantitative interpretation of the results since the subtraction of $\langle S_i^z \rangle_{3/2^+}$ will produce more complicated effects than just the cancellation of the contribution from the free chain-end spins at the sites 1 and L . However, one can still differ between extended and localized states. We found that the two states $3/2^-$ and $5/2^+$ clearly were localized around the impurity site for $J' = 0.2J$ whereas the state $5/2^-$ was extended.

We can now calculate the low-lying excitations as a function of coupling to the $s = 1/2$ impurity. Our results are shown in Fig. 10. The symbols denote the gaps: $E_{5/2^-} - E_{3/2^+}$ (triangles) to the state $5/2^-$ (Haldane gap), $E_{5/2^+} - E_{3/2^+}$ (squares) to the state $5/2^+$, and $E_{3/2^-} - E_{3/2^+}$ (filled squares) to the state $3/2^-$. The solid line is the Haldane gap, $\Delta E = 0.41050J$. The dashed line is the perturbative result Eq. (4.2), and the dot-dashed line Eq. (4.3). For small J' we see excellent agreement with the perturbative results. For $J' < J'_{c1} \approx 0.45J$ a bound state, calculated from the $3/2^-$ level, appears, and for $J' < J'_{c2} \approx 0.35J$ also bound state, calculated from the $5/2^+$ level, is stable.

B. Strong Coupling

As before, we try to arrive at an effective Hamiltonian capable of describing the low energy excitations. Again we shall assume that the coupling to the $s = 1/2$ impurity spin, J' , is always positive corresponding to an antiferromagnetic coupling. As a starting point we consider the three central spins $\mathbf{S}_{L/2}$, $\mathbf{S}_{L/2+1}$ and \mathbf{S}' , the $s = 1/2$ impurity. Disregarding the rest of the chain, these three spins will be described by a Hamiltonian

$$H_{\text{imp}} = J'[\mathbf{S}_{L/2} \cdot \mathbf{S}' + \mathbf{S}' \cdot \mathbf{S}_{L/2+1}] \quad (4.4)$$

The spectrum of H_{imp} is as follows: The ground-state is a quadruplet $S^P = 3/2^+$ with $E = -3/2J'$, then a doublet $S^P = 1/2^-$ with $E = -1J'$, another doublet $S^P = 1/2^+$ with $E = 0$, a quadruplet $S^P = 3/2^-$ with $E = J'/2$ and finally a sextuplet $S^P = 5/2^+$ with energy $E = J'$. Since the ground-state of H_{imp} is a multiplet with $s = 3/2$, the effective Hamiltonian becomes that of an effective $s = 3/2$ impurity in the otherwise uniform AF $s = 1$ chain. If we by $\mathcal{P}^{(3/2)}$ denote the projection onto the $s = 3/2$ ground-state subspace of H_{imp} , we can write $\mathcal{P}^{(3/2)}\mathbf{S}_{L/2}\mathcal{P}^{(3/2)} = \beta\mathbf{S}_{s=3/2}''$. The effective Hamiltonian can then be written:

$$H_{\text{eff}} = J \sum_{i=1}^{L/2-2} \mathbf{S}_i \cdot \mathbf{S}_{i+1} + J \sum_{i=L/2+2}^{L-1} \mathbf{S}_i \cdot \mathbf{S}_{i+1} + H_{\text{imp}}(s = 3/2), \quad (4.5)$$

where the term describing the $s = 3/2$ impurity is given by:

$$\begin{aligned} H_{\text{imp}}(s = 3/2) &= J[\mathbf{S}_{L/2-1} \cdot \mathcal{P}^{(3/2)}\mathbf{S}_{L/2}\mathcal{P}^{(3/2)} + \mathcal{P}^{(3/2)}\mathbf{S}_{L/2+1}\mathcal{P}^{(3/2)} \cdot \mathbf{S}_{L/2+2}] \\ &= \beta J[\mathbf{S}_{L/2-1} \cdot \mathbf{S}_{s=3/2}'' + \mathbf{S}_{s=3/2}'' \cdot \mathbf{S}_{L/2+2}]. \end{aligned} \quad (4.6)$$

Here $\mathbf{S}_{s=3/2}''$ denotes the effective $s = 3/2$ spin. We need to determine β . We begin by writing down the matrices for $S_{L/2}^z$ and $S_{L/2+1}^z$ projected onto the $3/2^+$ ground-state subspace of H_{imp} . These have to be proportional to a spin-3/2 representation. We find:

$$\langle \frac{3}{2} | S_{L/2}^z | \frac{3}{2} \rangle = \langle \frac{3}{2} | S_{L/2+1}^z | \frac{3}{2} \rangle = \begin{pmatrix} \frac{9}{10} & 0 & 0 & 0 \\ 0 & \frac{3}{10} & 0 & 0 \\ 0 & 0 & -\frac{3}{10} & 0 \\ 0 & 0 & 0 & -\frac{9}{10} \end{pmatrix}. \quad (4.7)$$

Clearly, this is just $(3/5)S_{s=3/2}^z$, as expected. Thus, if we project $\mathbf{S}_{L/2}$ and $\mathbf{S}_{L/2+1}$ onto the $3/2^+$ subspace we get in both cases a result proportional to a spin-3/2 by a factor $3/5$, i.e. $(3/5)\mathbf{S}_{s=3/2}$. Thus,

$$\beta = 3/5. \quad (4.8)$$

The coupling to the $s = 3/2$ impurity is therefore fixed at $J3/5$.

Let us consider the more general case where we instead of Eq. (4.6) have

$$H_{\text{imp}}(s = 3/2) = K[\mathbf{S}_{L/2-1} \cdot \mathbf{S}_{s=3/2}'' + \mathbf{S}_{s=3/2}'' \cdot \mathbf{S}_{L/2+2}], \quad (4.9)$$

i. e. we regard the coupling to the $s = 3/2$ impurity as a free parameter, K . We would expect bound states to appear for $K < K_c^{(3/2)}$. For very small K , $K \ll K_c^{(3/2)}$, we could again assume that effective $s = 1/2$ chain-end spins on the sites $L/2 - 1$ and $L/2 + 2$ would be a valid description, and we would arrive at an effective low-energy Hamiltonian consisting only of the two chain-end spins, and the $s = 3/2$ impurity:

$$H_{\text{eff}} = \alpha K[\mathbf{S}_{L/2-1}'' \cdot \mathbf{S}_{s=3/2}'' + \mathbf{S}_{s=3/2}'' \cdot \mathbf{S}_{L/2+2}''], \quad K \ll K_c^{(3/2)}. \quad (4.10)$$

Here, $\alpha \simeq 1.064$, and $\mathbf{S}_{L/2-1}'', \mathbf{S}_{L/2+2}''$ are $s = 1/2$ spins. The low-energy Hamiltonian, Eq. (4.10), has the following spectrum. A ground-state doublet with energy $E = -\alpha K 5/2$, an excited quadruplet at $E = -\alpha K$, another quadruplet at $E = 0$, and finally a sextuplet at $E = \alpha K 3/2$. For sufficiently small K all three bound states should be stable giving rise to energy levels in the Haldane gap given by the corresponding energy differences, $\alpha K 3/2$, $\alpha K 5/2$, and $\alpha K 4$.

Returning to the full effective Hamiltonian, Eq. (4.5), the question of whether bound states appear comes down to the question of whether $J3/5$ is below or above the threshold, $K_c^{(3/2)}$. As we shall see below, the numerical results indicate that $J3/5$ is too large for any bound states to be stable. It is then *not* possible to write down an effective low-energy Hamiltonian based on the $s = 1/2$ chain-end spins, as we did in Eq. (4.10), and it is necessary to work with the full effective Hamiltonian, Eq. (4.5), which, due to the size of the corresponding Hilbert space, is not very useful.

We have calculated the gap $E_{5/2+} - E_{3/2+}$ for $J/J' = 1, 0.2$, and 0.1 using the DMRG method. For large J' this is the lowest-lying excitation. The results are shown in Fig. 11. In this case the convergence to the thermodynamic limit is rather slow and we have difficulty extrapolating the results to a high accuracy, we therefore show the unextrapolated results for a 120 site chain. Here the solid squares are the DMRG results, and the solid line denotes the isotropic Haldane gap of $\Delta = 0.41050J$. In this case the DMRG method can be used for even very large J' . As is clearly evident from Fig. 11 we never observe any states in

the Haldane gap. A calculation of $E_{3/2-} - E_{3/2+}$ also didn't show any bound states in the Haldane gap. We therefore conclude that the coupling to the effective $s = 3/2$ impurity, $J3/5$, is too large for any bound states to appear.

We have also calculated the expectation value of the z-component of the spin for the values of $J/J' = 1, 0.2$, and 0.1 . Our results are shown in Fig. 12. The circles are the results for $J/J' = 1$, the squares for $J/J' = 0.2$ and the triangles for $J/J' = 0.1$. In order to differ between extended and localized states we have subtracted $\langle S_I^z \rangle_{3/2+}$. As opposed to Section III the spin configuration that we subtract, here $\langle S_I^z \rangle_{3/2+}$, is non-zero across the impurity making it difficult to give a quantitative interpretation of these results. However, clearly the state is in all cases extended over the whole length of the chain.

Thus, we conclude that for a strong antiferromagnetic coupling to the $s = 1/2$ impurity no bound states exists below the Haldane gap. The fact that DiTusa et al.¹⁶ observes such states, indicates that, the appropriate (AF) J' , for a simple linear chain Heisenberg model description of their results, should be rather small.

V. FERROMAGNETIC COUPLINGS

We have only performed the numerical DMRG calculations for antiferromagnetically coupled impurities. It would be interesting to repeat the calculation using ferromagnetic couplings. Due to the rather large amount of CPU time required we have not done this. Since we in our implementation of the DMRG method do not work with the total spin as a good quantum number, but only with it's z-component, ferromagnetic interactions are generally also more difficult to treat, due to the fact that the ground-state belongs to a different multiplet for even and odd $L/2$. However, the effective Hamiltonians we have obtained in the previous sections can be derived for a ferromagnetic coupled impurity in a straightforward way. Below we briefly discuss what one finds.

For a central bond that is *weak*, $|J'| \ll |J|$, and *ferromagnetic* in an otherwise antiferromagnetically coupled $s = 1$ chain, we expect the results of Sec. III A to still apply.

In particular Eq. (3.3) should still be correct. However, in this case the ground state of Eq. (3.2) is the triplet.

For a central bond that is *strong*, $|J'| \gg |J|$, and *ferromagnetic*, the two central spins, $\mathbf{S}_{L/2}$ and $\mathbf{S}_{L/2+1}$, will have a $s = 2$ ground-state. We then obtain an effective Hamiltonian in terms of an effective $s = 2$ impurity:

$$H_{\text{eff}} = J \sum_{i=1}^{L/2-2} \mathbf{S}_i \cdot \mathbf{S}_{i+1} + J \sum_{i=L/2+2}^{L-1} \mathbf{S}_i \cdot \mathbf{S}_{i+1} + H_{\text{imp}}(s=2), \quad (5.1)$$

where the term describing the $s = 2$ impurity is given by:

$$\begin{aligned} H_{\text{imp}}(s=2) &= J[\mathbf{S}_{L/2-1} \cdot \mathcal{P}^{(2)} \mathbf{S}_{L/2} \mathcal{P}^{(2)} + \mathcal{P}^{(2)} \mathbf{S}_{L/2+1} \mathcal{P}^{(2)} \cdot \mathbf{S}_{L/2+2}] \\ &= \gamma J[\mathbf{S}_{L/2-1} \cdot \mathbf{S}_{s=2}'' + \mathbf{S}_{s=2}'' \cdot \mathbf{S}_{L/2+2}]. \end{aligned} \quad (5.2)$$

Here γ is determined by the projection of $\mathbf{S}_{L/2}$ and $\mathbf{S}_{L/2+1}$ onto the $s = 2$ subspace, $\mathcal{P}^{(2)} \mathbf{S}_{L/2} \mathcal{P}^{(2)} = \gamma \mathbf{S}_{s=2}''$. It is easy to see that $\gamma = 1/2$, thus, the effective coupling to the $s = 2$ impurity is $J/2$. If the coupling to the $s = 2$ impurity is regarded as a free parameter we would expect bound states to appear below a threshold, $K_c^{(2)}$. However, in the absence of any numerical data, we have no way of telling whether $J/2$ is above or below such a threshold and we cannot draw any conclusions. Let us briefly consider the case where the coupling to the $s = 2$ impurity is assumed to be a free variable K . For $K \ll K_c^{(2)}$ we can again use the picture of effective $s = 1/2$ chain-end spins to write an effective low-energy Hamiltonian: $H_{\text{eff}} = \alpha K[\mathbf{S}_{L/2-1}'' \cdot \mathbf{S}_{s=2}'' + \mathbf{S}_{s=2}'' \cdot \mathbf{S}_{L/2+2}'']$. As in previous sections, $\mathbf{S}_{L/2-1}''$ and $\mathbf{S}_{L/2+2}''$ are now effective $s = 1/2$ spins. This low-energy effective Hamiltonian has the following spectrum: A ground-state triplet with energy $E = -\alpha K 3$, followed by a quintuplet at $E = -\alpha K$, another quintuplet at $E = 0$, and finally a septuplet at $E = \alpha K 2$. For sufficiently small K , $K \ll K_c^{(2)}$, we then expect bound states in the Haldane gap to occur at energies, $2K\alpha$, $3K\alpha$, and $5K\alpha$. The effective Hamiltonian, Eq. (5.1), corresponds to $K = J/2$, since this is not a small coupling, a low-energy Hamiltonian based on the $s = 1/2$ chain-end spins is presumably not valid. Since we do not know $K_c^{(2)}$, it is not possible to tell if bound states occur.

If a $s = 1/2$ impurity is coupled with a *weak ferromagnetic* bond to the otherwise antiferromagnetically coupled $s = 1$ chain, we expect bound states to occur. As already mentioned in Sec. IV A, we expect these to have energies $\Delta E_{1/2-} = \alpha J'/2$, $\Delta E_{1/2+} = \alpha J'3/2$, with $\alpha \simeq 1.064$.

For a $s = 1/2$ impurity coupled with a *strong ferromagnetic* bond to an otherwise uniform $s = 1$ chain, we know from Sec. IV B that, the ground state of H_{imp} , Eq. (4.4) should be a sextuplet, $S^P = 5/2^+$. If we by $\mathcal{P}^{(5/2)}$ denote projection onto the $5/2$ subspace, we can define a constant, δ , by $\mathcal{P}^{(5/2)}\mathbf{S}_{L/2}\mathcal{P}^{(5/2)} = \delta\mathbf{S}_{s=5/2}''$. We can then write an effective Hamiltonian in terms of an effective $s = 5/2$ impurity in the following way:

$$H_{\text{eff}} = J \sum_{i=1}^{L/2-2} \mathbf{S}_i \cdot \mathbf{S}_{i+1} + J \sum_{i=L/2+2}^{L-1} \mathbf{S}_i \cdot \mathbf{S}_{i+1} + H_{\text{imp}}(s = 5/2), \quad (5.3)$$

where the term describing the $s = 5/2$ impurity is given by:

$$\begin{aligned} H_{\text{imp}}(s = 5/2) &= J[\mathbf{S}_{L/2-1} \cdot \mathcal{P}^{(5/2)}\mathbf{S}_{L/2}\mathcal{P}^{(5/2)} + \mathcal{P}^{(5/2)}\mathbf{S}_{L/2+1}\mathcal{P}^{(5/2)} \cdot \mathbf{S}_{L/2+2}] \\ &= \delta J[\mathbf{S}_{L/2-1} \cdot \mathbf{S}_{s=5/2}'' + \mathbf{S}_{s=5/2}'' \cdot \mathbf{S}_{L/2+2}]. \end{aligned} \quad (5.4)$$

In this case $\delta = 2/5$. The effective coupling to the $s = 5/2$ impurity is then $2J/5$. If we regard this coupling as a free parameter, K , we expect bound states to occur for K below a threshold, $K_c^{(5/2)}$. We are not able to determine if $2J/5$ is below such a threshold. As above, let us consider the case where the coupling to the $s = 5/2$ impurity is a free variable K . For $K \ll K_c^{(5/2)}$ we can again use the picture of effective $s = 1/2$ chain-end spins to write an effective low-energy Hamiltonian: $H_{\text{eff}} = \alpha K[\mathbf{S}_{L/2-1}'' \cdot \mathbf{S}_{s=5/2}'' + \mathbf{S}_{s=5/2}'' \cdot \mathbf{S}_{L/2+2}'']$. As above, $\mathbf{S}_{L/2-1}''$ and $\mathbf{S}_{L/2+2}''$ are now effective $s = 1/2$ spins. This low-energy effective Hamiltonian has the following spectrum: A ground-state quadruplet with energy $E = -\alpha K7/2$, followed by a sextuplet at $E = -\alpha K$, another sextuplet at $E = 0$, and finally an octuplet at $E = \alpha K5/2$. For sufficiently small K we then expect bound states in the Haldane gap to occur at energies, $\alpha K5/2$, $\alpha K7/2$, and $\alpha K6$. The effective Hamiltonian, Eq. (5.3), corresponds to $K = 2J/5$, this coupling cannot be regarded as small and we are not in the regime $K \ll K_c^{(5/2)}$. Thus, the description based on the $s = 1/2$ chain-end spins is of limited use. However, whether

$2J/5$ is below or above $K_c^{(5/2)}$ is an open question.

We see that only in specific cases is it straight forward to derive a useful *low-energy* effective Hamiltonian. For a strong ferromagnetic bond, and for a $s = 1/2$ impurity coupled with a *strong ferromagnetic* bond, further numerical work will be needed in order to determine whether bound states in the Haldane gap exists.

VI. DISCUSSION

We have shown that, by the introduction of an AF bond with $J' \neq J, J' \geq 0$ in an otherwise isotropic AF $s = 1$ chain, a triplet bound state below the Haldane gap occurs for sufficiently large and small J' . The energy of the bound state is in very good agreement with perturbative results based on effective $s = 1/2$ chain-end excitations created by broken valence bonds. In a region $0.7J \approx J'_{\text{c weak}} \leq J' \leq J'_{\text{c strong}} \approx 2.0J$ no bound state is found to within numerical precision. If a $s = 1/2$ impurity is introduced with an AF coupling $J' \neq J, J' \geq 0$ in an isotropic AF $s = 1$ chain we find that, only for J' below $J'_{\text{c 1}} \approx 0.45J$ do bound states occur. For $J' < J'_{\text{c 1}} \approx 0.45J$ a bound state appears, and for $J' < J'_{\text{c 2}} \approx 0.35J$ a second bound state is stable. At large impurity couplings, $J' > J$, we find no bound states.

In experiments on $\text{Y}_{2-x}\text{Ca}_x\text{BaNiO}_5$ ¹⁶, states below the Haldane gap have been found. In a simple linear chain spin model of $\text{Y}_{2-x}\text{Ca}_x\text{BaNiO}_5$, our results would imply that the coupling to a $s = 1/2$ impurity, introduced by the Ca doping, should be rather small, if it is antiferromagnetic. This may seem surprising since we would expect $|J'| > |J|$ to be the more likely scenario in $\text{Y}_{2-x}\text{Ca}_x\text{BaNiO}_5$. However, the coupling could be large and *ferromagnetic* in which case we cannot rule out the existence of bound states. Secondly, the non-zero single ion anisotropy term, $D(S_i^z)^2$, relevant for $\text{Y}_{2-x}\text{Ca}_x\text{BaNiO}_5$ could create bound states in the gap even for a large antiferromagnetic coupling to the $s = 1/2$ impurity. Also, the substitution of Y^{3+} by Ca^{2+} will lower the crystal field symmetry on close by Ni sites, justifying new *local* anisotropy terms in a spin Hamiltonian. Possibly such terms could create bound states. DiTusa et al.¹⁶ argue that the magnetic disturbance caused by

the Ca doping introduces either a triplet or a quartet of subgap bound states. Our results indicate that several different multiplets of bound states are likely to be present, some of which have spin larger than $1/2$, even for the simple scenario of Ca doping giving rise to $s = 1/2$ impurities, thus justifying the large contribution to the spectral weight from the impurities seen in the experiments.

Our finding that a critical coupling is needed to form bound states in this problem may seem surprising at first, since one would expect that even an infinitely small impurity potential would form a bound state in one dimension. However, in a $NL\sigma$ model description one can argue that the introduction of impurities do not give rise to simple local potentials due to the constraint $|\phi|^2 = 1$. This might change in a model where the rotational symmetry is broken by the introduction of a single ion anisotropy term, $D(S_i^z)^2$. Such a term is relevant for the description of NENP and Y_2BaNiO_5 . It would therefore be very interesting to repeat the above DMRG calculations with $D \neq 0$.

ACKNOWLEDGMENTS

We gratefully acknowledge many enlightning discussions with W. J. L. Buyers. One of us (ESS) would like to thank C. Broholm, D. Reich, R. Hyman, S. M. Girvin and A. Macdonald for useful discussions and comments. ESS is supported by NSF grant number NSF DMR-9416906. This research was supported in part by NSERC of Canada.

REFERENCES

- ¹ F. D. M. Haldane, Phys. Lett. **93A**, 464 (1983); Phys. Rev. Lett. **50**, 1153 (1983).
- ² W. J. L. Buyers, R. M. Morra, R. L. Armstrong, M. J. Hogan, P. Gerlach, and K. Hirikawa, Phys. Rev. Lett. **56**, 371 (1986).
- ³ J. P. Renard, M. Verdaguer, L.P. Regnault, W. A. C. Erkelens, J. Rossat-Mignod, and W. G. Stirling, Europhys. Lett. **3**, 945 (1987).
- ⁴ R. Botet and R. Julien, Phys. Rev. B **27**, 613, (1983); R. Botet, R. Julien, and M. Kolb, Phys. Rev. B **28**, 3914 (1983); M. Kolb, R. Botet, and R. Julien, J. Phys. A **16** L673 (1983); M. P. Nightingale and H. W. J. Blöte, Phys. Rev. B **33**, 659 (1986); H. J. Schulz and T. A. L. Ziman, Phys. Rev. B **33**, 6545 (1986).
- ⁵ S. R. White and D. A. Huse, Phys. Rev. B **48**, 3844 (1993).
- ⁶ O. Golinelli, Th. Jolicœur, and R. Lacaze, Phys. Rev. B **50**, 3037 (1994).
- ⁷ O. Golinelli, Th. Jolicœur, and R. Lacaze, Phys. Rev. B **46**, 10854 (1992); J. Phys. Cond. Matt. **5**, 1399 (1994). S. Haas, J. Riera, and E. Dagotto, Phys. Rev. B **48**, 3281 (1993); M. Takahashi, Phys. Rev. B **48**, 311 (1993); **50**, 3045 (1994).
- ⁸ J. P. Renard, M. Verdaguer, L.P. Regnault, W. A. C. Erkelens, J. Rossat-Mignod, J. Ribas, W. G. Stirling, and C. Vettier, J. Appl. Phys. **63**, 3538 (1988); W. Lu, J. Tuchendler, M. von Ortenberg, and J. P. Renard, Phys. Rev. Lett. **67**, 3716 (1991); L. P. Regnault, C. Vettier, J. Rossat-Mignod, and J. P. Renard, Physica B **180-181**, 188 (1992); L. C. Brunel, T. M. Brill, I. Zaliznyak, J. P. Boucher, and J. P. Renard, Phys. Rev. Lett. **69**, 1699 (1992); S. Ma, C. Broholm, D. H. Reich, B. J. Sternlieb, and R. W. Erwin, Phys. Rev. Lett. **69**, 3571 (1992); W. Palme, H. Kriegelstein, B. Lüthi, T. M. Brill, T. Yosida, M. Date, Int. J. Mod. Phys. B **7**, 1016 (1993).
- ⁹ O. Golinelli, Th. Jolicœur, and R. Lacaze, Phys. Rev. B **45**, 9798 (1992).

- ¹⁰ J. Amador, E. Gutiérrez-Puebla, M. A. Mongo, I. Rasines, C. Ruíz-Valero, F. Fernández, R. Sáez-Puche, and J. A. Campá, Phys. Rev. B **42**, 7918 (1990).
- ¹¹ R. Sáez-Puche, J. M. Coronado, C. L. Otero-Díaz, and J. M. Martín Llorente, J. Solid State Chem. **93**, 461 (1991).
- ¹² D. J. Buttrey, J. D. Sullivan, and A. L. Rheingold, J. Solid State Chem. **88**, 291 (1990).
- ¹³ J. Darriet and L. P. Regnault, Solid State Commun. **86**, 409 (1993).
- ¹⁴ B. Batlogg, S.-W. Cheong, and L. W. Rupp, Jr. Physica B **194-196**, 173 (1994).
- ¹⁵ J. F. DiTusa, S.-W. Cheong, C. Broholm, G. Aeppli, L. W. Rupp, Jr., and B. Batlogg, Physica B **194-196**, 181 (1994).
- ¹⁶ J. F. Ditusa, S.-W. Cheong, J.-H. Park, G. Aeppli, C. Broholm and C. T. Chen, Phys. Rev. Lett. **73**, 1857 (1994).
- ¹⁷ A. P. Ramirez, S.-W. Cheong and M. L. Kaplan, Phys. Rev. Lett. **72**, 3108 (1994).
- ¹⁸ I. Affleck, T. Kennedy, E. H. Lieb, and H. Tasaki, Phys. Rev. Lett. **59**, 799 (1987); Commun. Math. Phys. **115**, 477 (1988).
- ¹⁹ M. Hagiwara, K. Katsumata, I. Affleck, B. I. Halperin, and J. P. Renard, Phys. Rev. Lett. **65**, 3181 (1990); M. Hagiwara, K. Katsumata, H. Hori, T. Takeuchi, M. Date, A. Yamagishi, J. P. Renard, and I. Affleck, Physica B **177**, 386 (1992); M. Hagiwara, K. Katsumata, J. P. Renard, I. Affleck, and B. I. Halperin, J. Mag. Mag. Mat. **104**, 839 (1992).
- ²⁰ S. H. Glarum, S. Geschwind, K. M. Lee, M. L. Kaplan, and J. Michel, Phys. Rev. Lett. **67**, 1614 (1991).
- ²¹ S. R. White and R. M. Noack, Phys. Rev. Lett. **68**, 3487 (1992).
- ²² S. R. White, Phys. Rev. Lett. **69**, 2863 (1992).

- ²³ S. R. White, Phys. Rev. B **48**, 10345 (1993).
- ²⁴ P. P. Mitra, B. I. Halperin, and I. Affleck, Phys. Rev. B **45**, 5299 (1992).
- ²⁵ E. S. Sørensen and I. Affleck, Phys. Rev. B **49**, 15771 (1994).
- ²⁶ E. S. Sørensen and I. Affleck, Phys. Rev. Lett. **71**, 1633 (1993).
- ²⁷ B. Simon, Ann. Phys. **97**, 279 (1976).
- ²⁸ I. Affleck, Phys. Rev. Lett. **62**, 474, E 1927 (1989); **65**, 2477, 2835 (1990); Phys. Rev. B **41**, 6697 (1990); **43**, 3215 (1991); I. Affleck and R. A. Weston, *ibid.* **45**, 4667 (1992).
- ²⁹ Z.-Y. Lu, Z.-B. Su, and L. Yu, preprint 1994.
- ³⁰ A. Aharony, R. J. Birgenau, A. Coniglio, M. A. Kastner, H. E. Stanley, Phys. Rev. Lett. **60**, 1330 (1988).

FIGURES

FIG. 1. Schematic picture of the two different perturbations. In a) is shown the perturbed bond with coupling strength J' at the center of a $s = 1$ chain with coupling J . In b) is shown the $s = 1/2$ impurity coupled with coupling strength J' to the rest of the $s = 1$ chain.

FIG. 2. The energy gap $\Delta E(L) = E_{2+}(L) - E_{1-}(L)$ as a function of chain length, L , for a weak bond, $J'/J = 0.1$. The limiting value of the gap is 0.11405.

FIG. 3. The bound state in real space for a chain with $L = 100$. $\langle S_i^z \rangle_{2+} - \langle S_i^z \rangle_{1-}$ for a weak bond, $J'/J = 0.1$. Clearly visible is the localized state around the impurity site.

FIG. 4. The energy gap, $\Delta E = E_{2+} - E_{1-}$ (solid squares), as a function of the weak perturbed bond, J'/J . The solid line is the isotropic Haldane gap, $\Delta/J = 0.41050$. The dashed line indicates the perturbative result, Eq. (3.3).

FIG. 5. $\langle S_i^z \rangle_{2+} - \langle S_i^z \rangle_{1-}$ as function of chain index i for a weak bond, $J'/J = 0.7$, close to the critical coupling.

FIG. 6. The energy gap $\Delta E = E_{2+} - E_{1-}$ as a function of the strong perturbed bond, J/J' . The solid squares are the DMRG results. The solid line is the isotropic Haldane gap, $\Delta/J = 0.41050$. The dashed line indicates the perturbative result, Eq. (3.13). The open circles denote exact diagonalization results of Eq. (3.4).

FIG. 7. The bound state in real space for a chain with $L = 100$. $\langle S_i^z \rangle_{2+} - \langle S_i^z \rangle_{1-}$ as a function i for a strong bond, $J/J' = 0.25$. The quenched singlet right at the center of the chain is clearly visible.

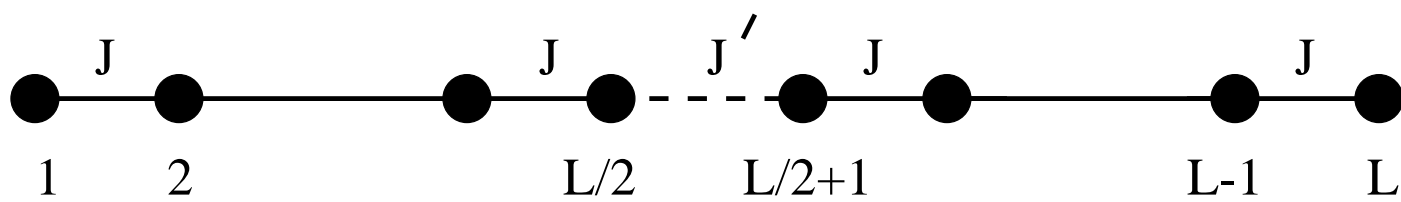
FIG. 8. The low-lying levels for a weakly antiferromagnetically coupled $s = 1/2$ in a spin-one chain.

FIG. 9. The energy gap, $\Delta E(L)$, as a function of chain length L , for a $s = 1$ chain with a $s = 1/2$ impurity. The coupling to the $s = 1/2$ is $J' = 0.2J$. The symbols denote the gaps: $E_{5/2-}(L) - E_{3/2+}(L)$ (triangles) to the state $5/2^-$ (Haldane gap), $E_{5/2+}(L) - E_{3/2+}(L)$ (squares) to the state $5/2^+$, and $E_{3/2-}(L) - E_{3/2+}(L)$ (circles) to the state $3/2^-$.

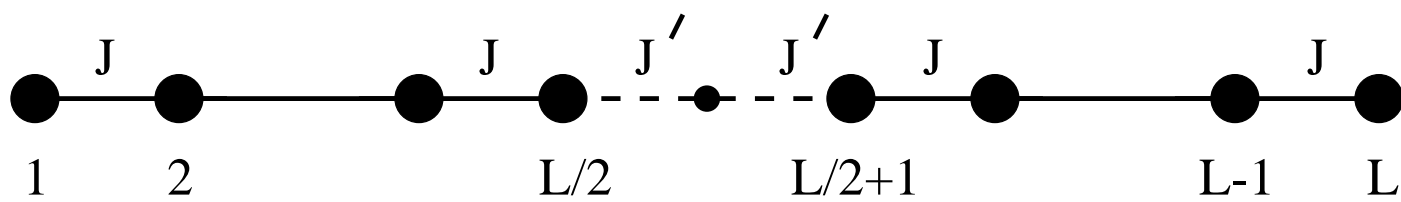
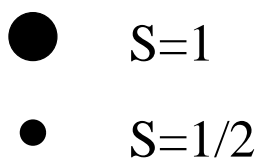
FIG. 10. The low-lying excitations as a function of coupling, J/J' , to a weakly coupled $s = 1/2$ impurity. The symbols denote the gaps: $E_{5/2-} - E_{3/2+}$ (triangles) to the state $5/2^-$ (Haldane gap), $E_{5/2+} - E_{3/2+}$ (squares) to the state $5/2^+$, and $E_{3/2-} - E_{3/2+}$ (filled squares) to the state $3/2^-$. The filled squares denote the DMRG results for a 120 site chain. The solid line is the Haldane gap, $\Delta E = 0.41050J$. The dashed line is the perturbative result, Eq. (4.2), and the dot-dashed line Eq. (4.3).

FIG. 11. The gap, $E_{5/2+} - E_{3/2+}$, as a function of coupling, J/J' , to the $s = 1/2$ impurity. The filled squares denote the DMRG results for a 120 site chain. No extrapolation to the thermodynamic limit has been performed. The solid line is the Haldane gap, $\Delta E = 0.41050J$.

FIG. 12. $\langle S_i^z \rangle_{5/2+} - \langle S_i^z \rangle_{1/2+}$ as a function i , for $J/J' = 1$ (circles), $J/J' = 0.2$ (squares), $J/J' = 0.1$ (triangles).



a)



b)

Fig 1. Sorensen, Affleck

Fig 2. Sorensen, Affleck

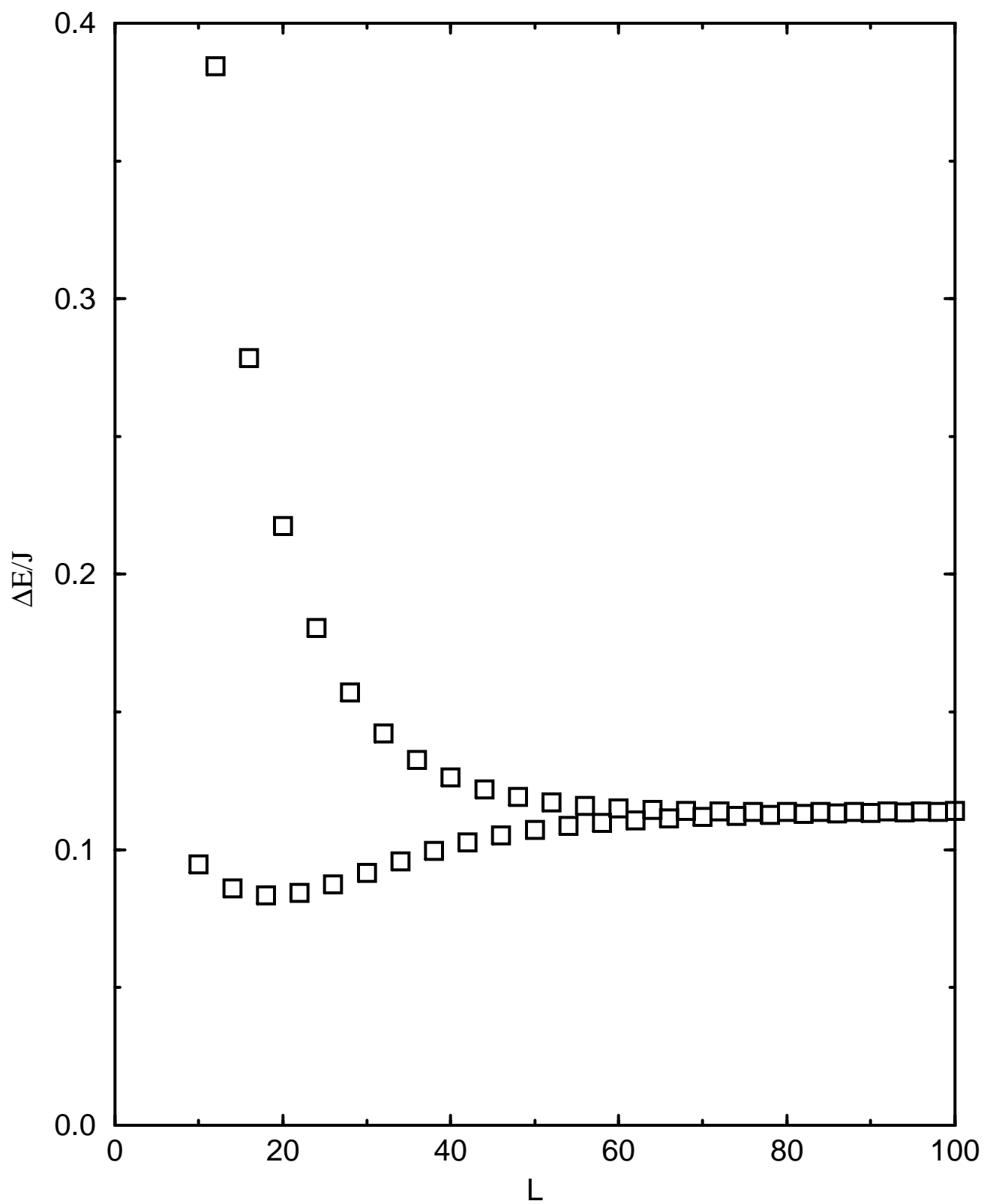


Fig 3. Sorensen, Affleck

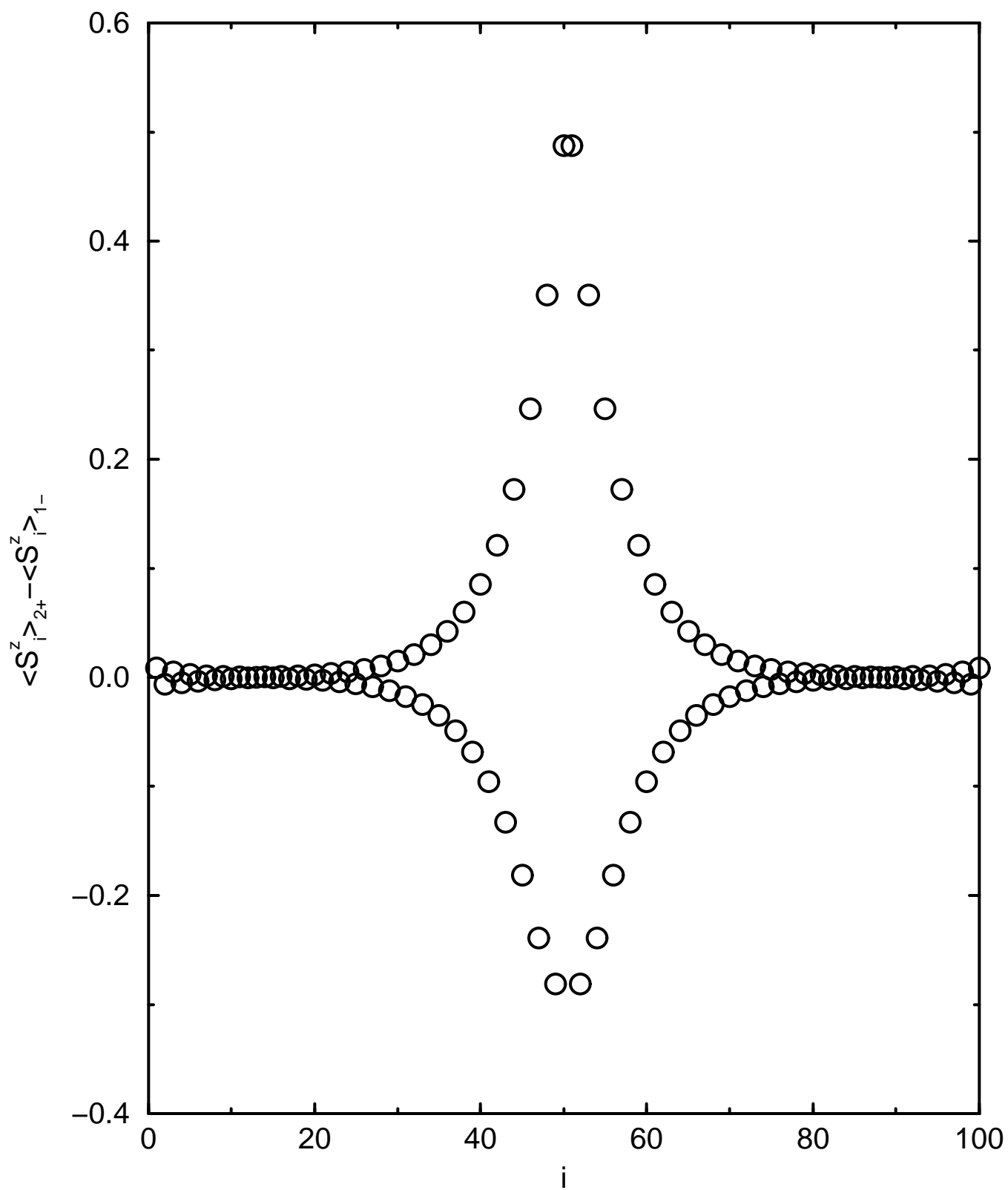


Fig. 4. Sorensen, Affleck

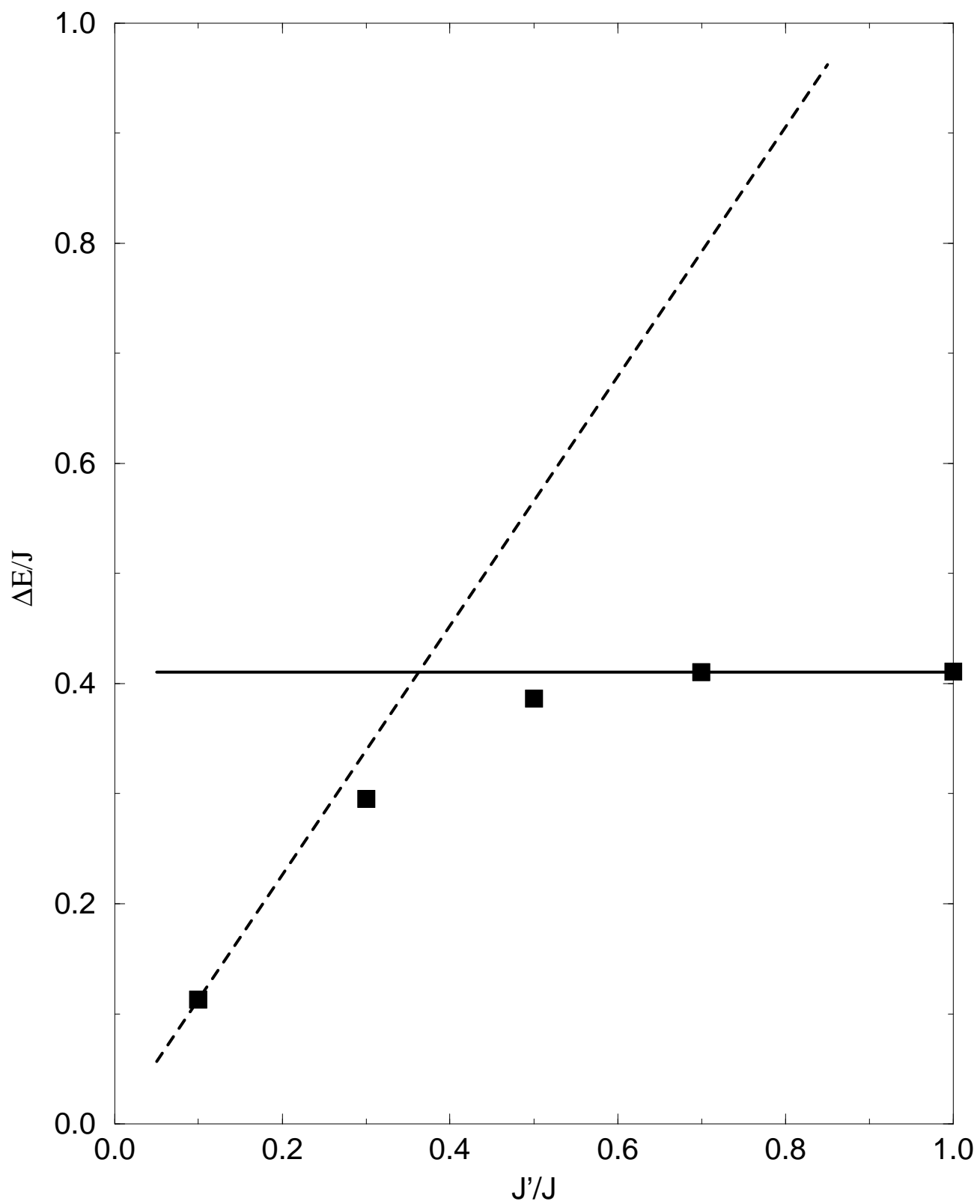


Fig. 5. Sorensen, Affleck

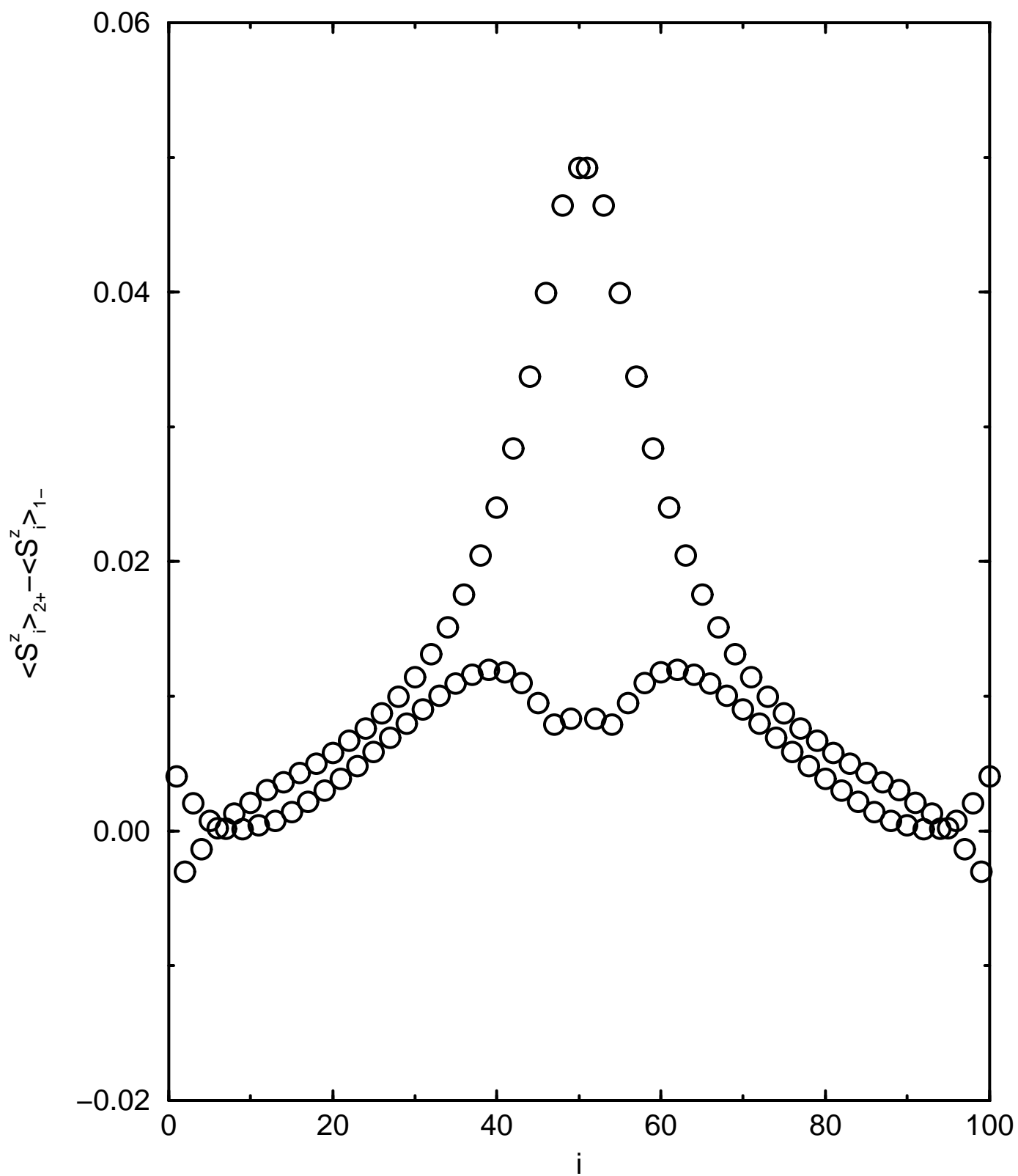


Fig. 6. Sorensen, Affleck

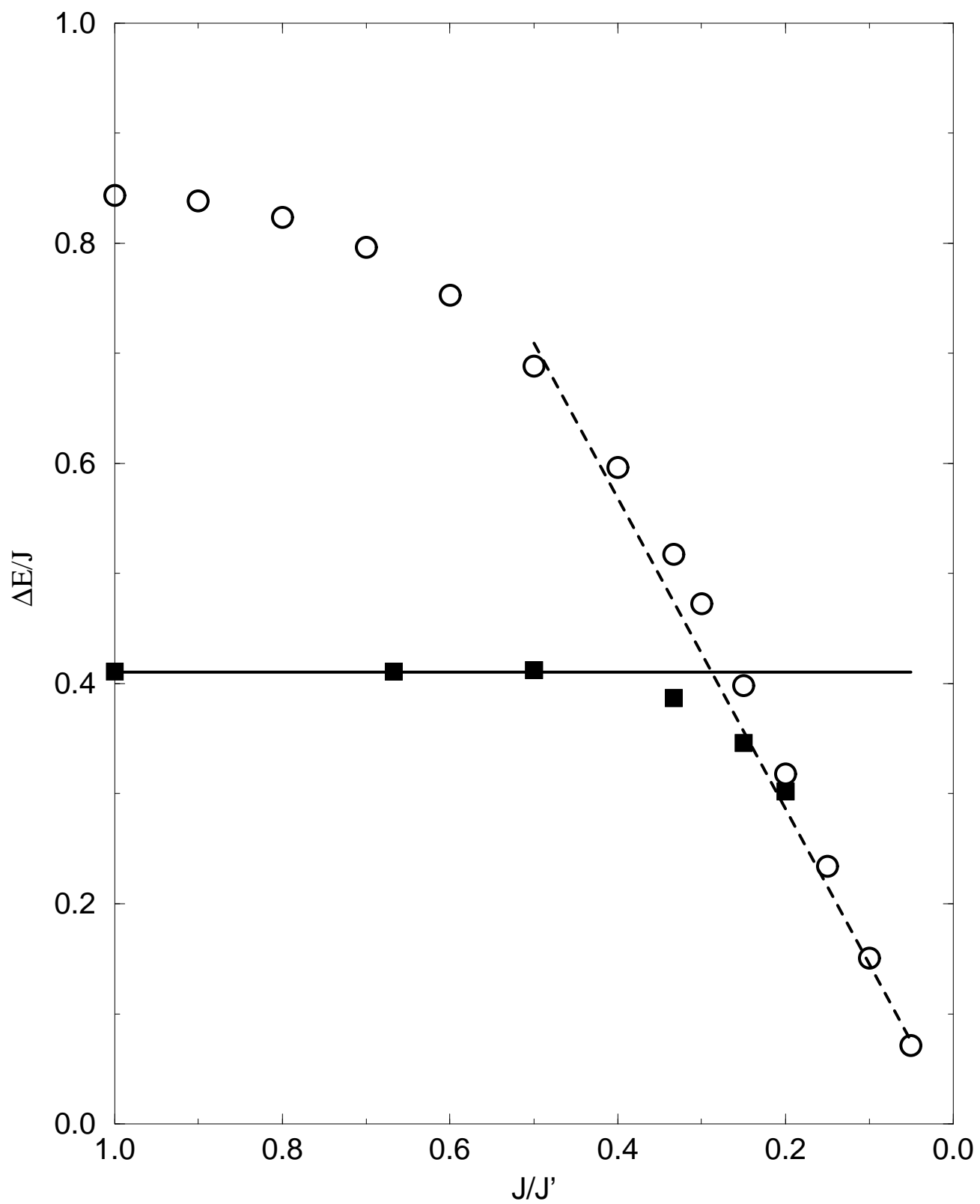
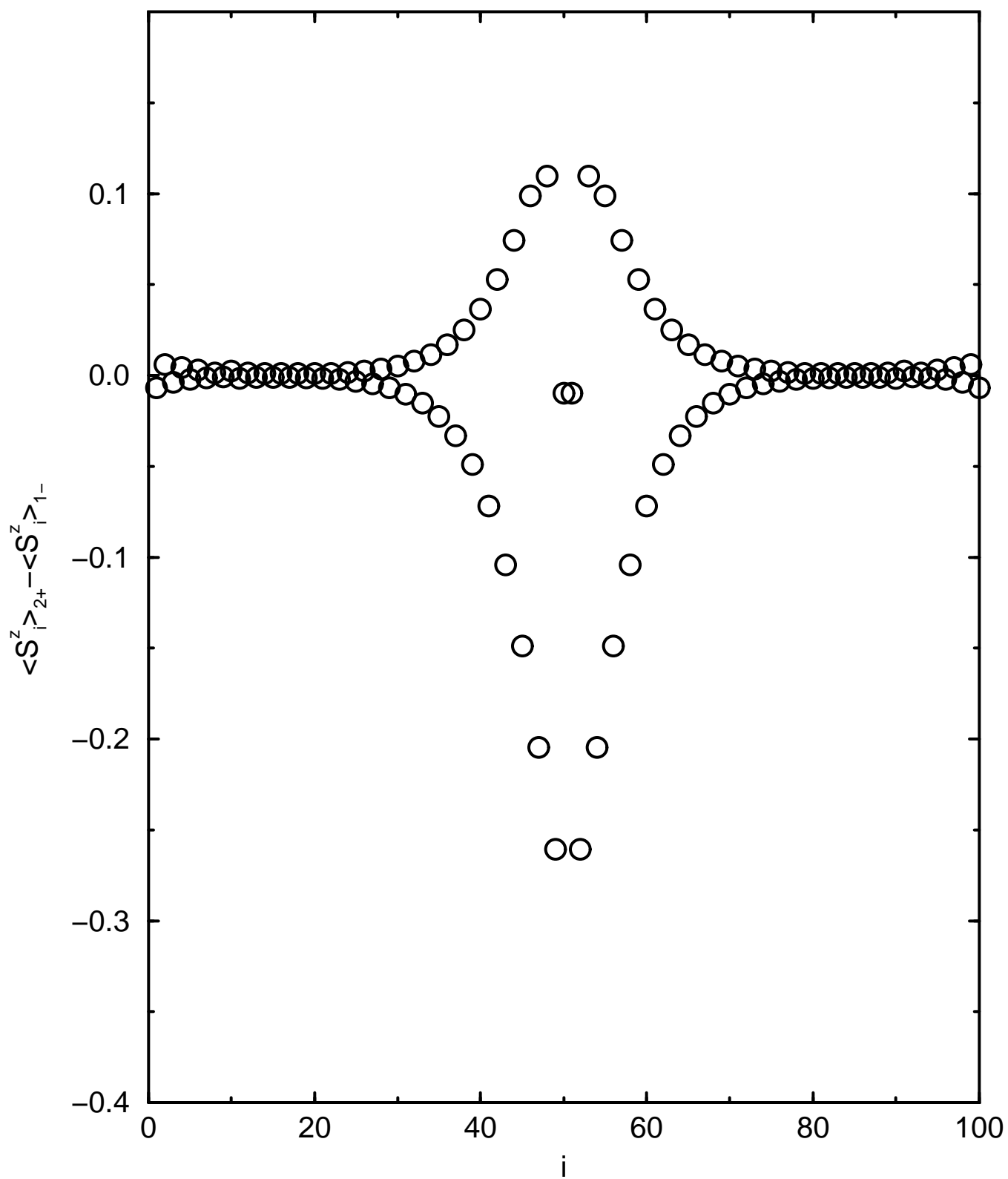
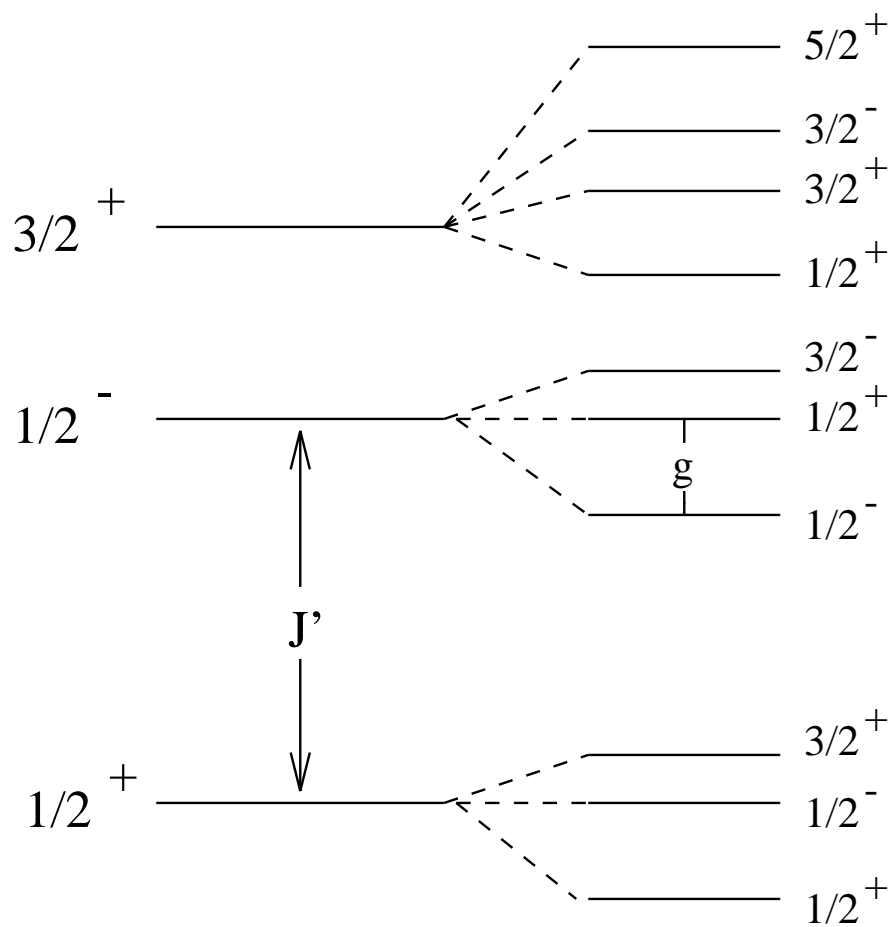
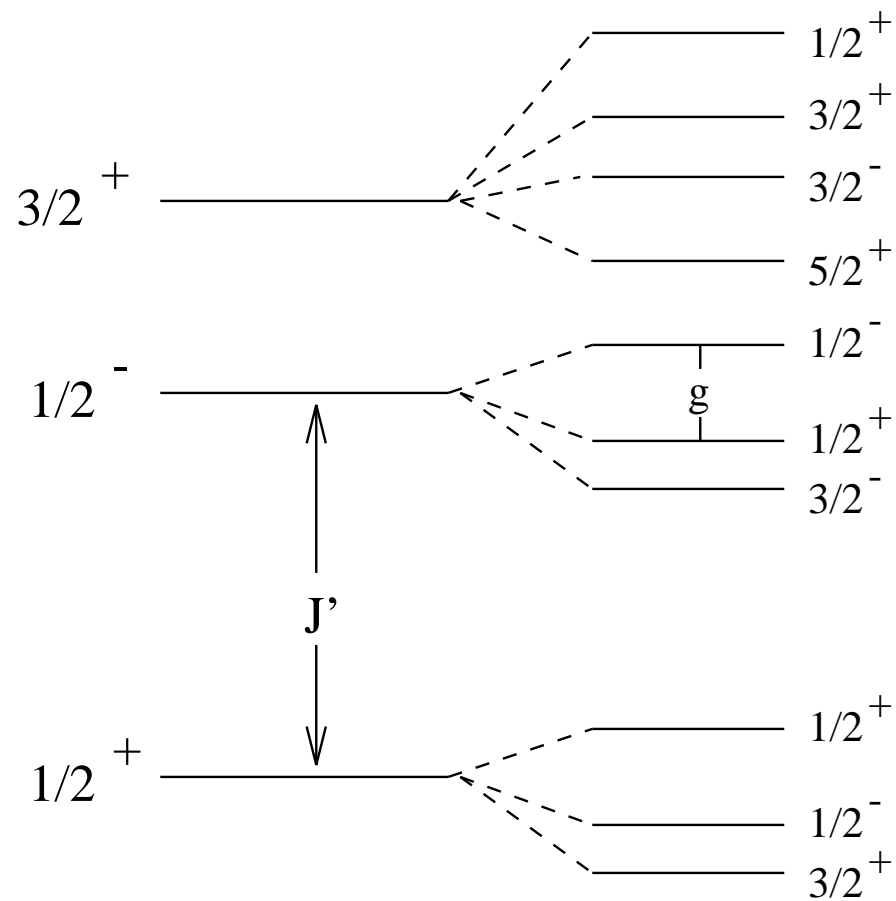


Fig. 7. Sorensen, Affleck





a) $L/2$ Even



$L/2$ Odd

Fig. 8. Sorensen, Affleck

Fig. 9. Sorensen, Affleck

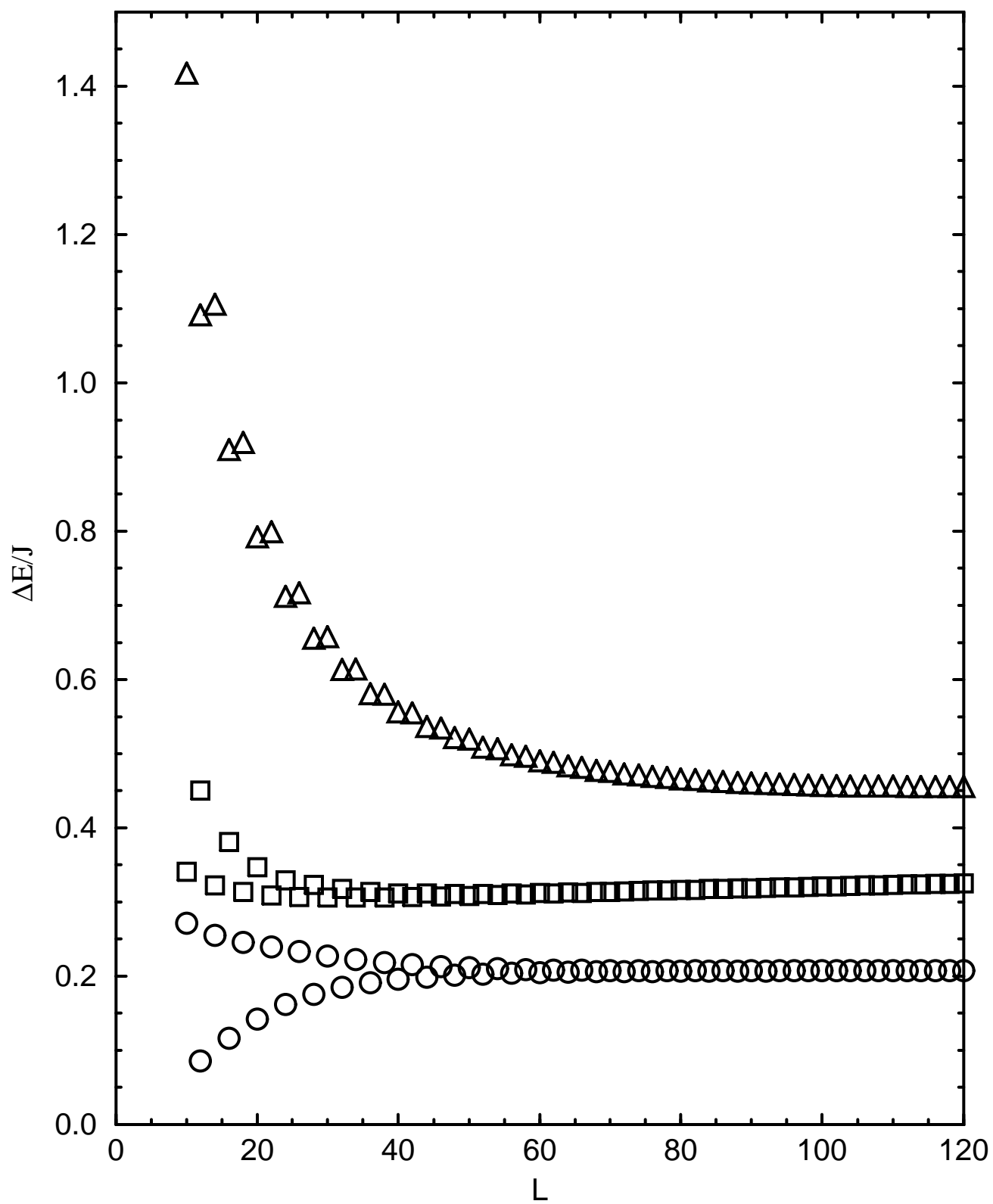


Fig. 10. Sorensen, Affleck

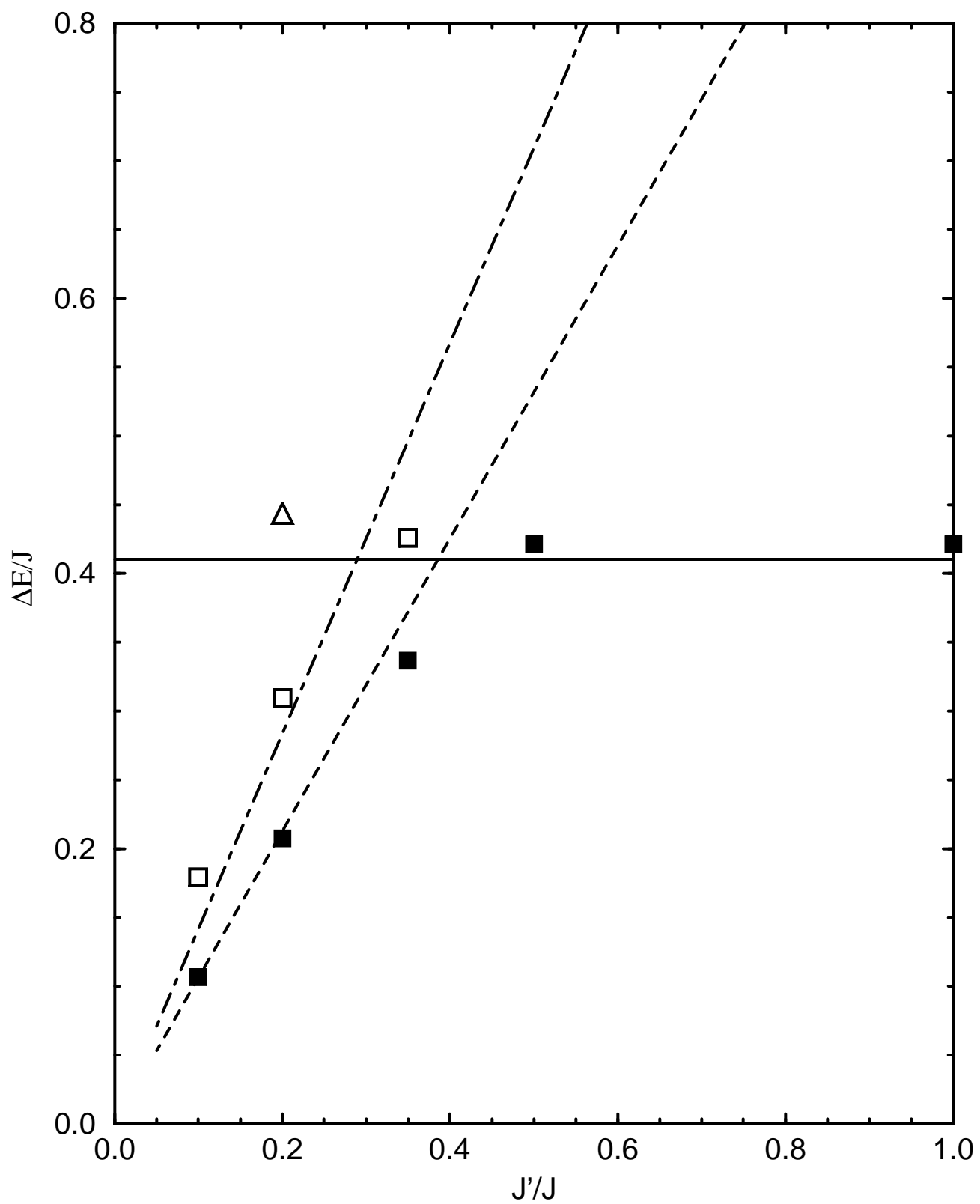


Fig. 11. Sorensen, Affleck

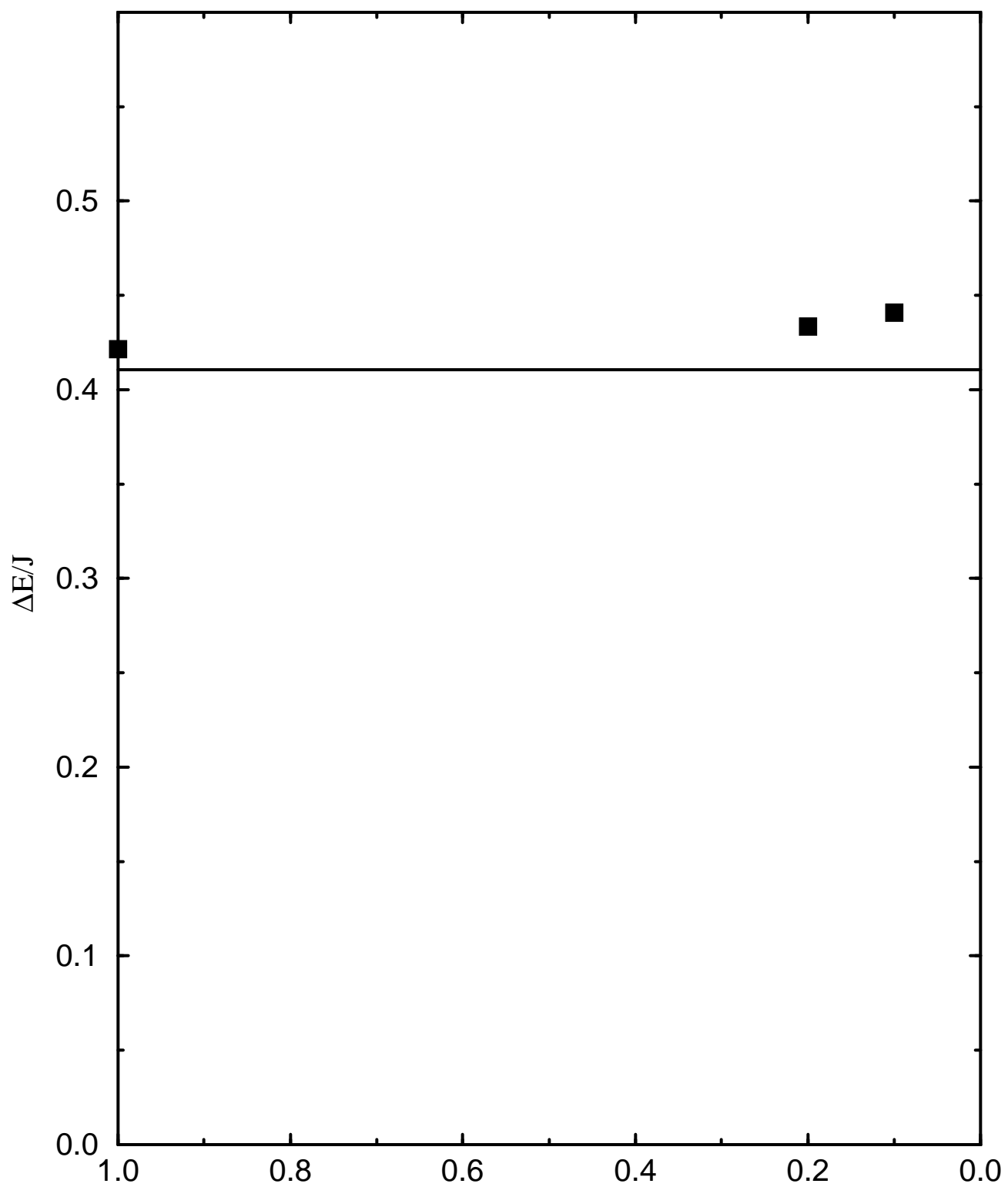


Fig. 12. Sorensen, Affleck

